ISSN 1063-7761, Journal of Experimental and Theoretical Physics, 2020, Vol. 130, No. 3, pp. 327–337. © Pleiades Publishing, Inc., 2020.
Russian Text © The Author(s), 2020, published in Zhurnal Eksperimental'noi i Teoreticheskoi Fiziki, 2020, Vol. 157, No. 3, pp. 394–405.

ATOMS, MOLECULES, OPTICS

Radiation from Elliptical Undulators with Magnetic Field Harmonics

A. M. Kalitenko[a] and K. V. Zhukovskii[a,*]

[a] *Moscow State University, Moscow, 119991 Russia*

**e-mail: zhukovsk@physics.msu.ru*

Received May 4, 2019; revised July 12, 2019; accepted July 12, 2019

Abstract—We analyze undulator radiation in some multiperiodic magnetic fields. We consider undulators with planar, helical, and elliptical axisymmetric magnetic fields with higher field harmonics. For these undulators, we obtain exact analytic expressions for generalized Bessel functions and Bessel coefficients. Analytic results are compared with the results of numerical simulation. We analyze the effect of additional third field harmonic on radiation emitted by these undulators. For a helical undulator with an additional asymmetric third harmonic field, it is found that the fifth harmonic of undulator radiation prevails over the third harmonic. We perform 3D simulation of radiation from free-electron laser with such an undulator using the specially developed numerical program that accounts for the electron energy spread in the beam as well as betatron oscillations. We analyze two-frequency undulator with a harmonic elliptically polarized magnetic field and simulate radiation of a free-electron laser with such an undulator.

DOI: 10.1134/S106377612001015X

1. INTRODUCTION

Undulator radiation (UR) is emitted by relativistic electrons moving in a periodic system of magnetic fields (undulator) and has the same origin as synchrotron radiation [1]. Ginzburg [2] was the first to put forth the idea of undulator. He also proposed a dynamic undulator in which an electron beam propagates in the time-varying field of an electromagnetic wave propagating in the two-wire line. Ginzburg considered radiation from a sequence of electron bunches with a longitudinal size smaller than the wavelength of generated radiation and emphasized that this radiation is coherent. Later, in the middle of the 20th century, Motz [3] proposed an undulator in the form of the amplifier for a free-electron laser (FEL) consisting of a sequence of dipole magnets with alternating polarities, which are arranged uniformly along the axis. At present, undulators and their radiation [4–8] are interesting in the context of their use in FELs in which the interaction of electrons with radiation groups electrons into bunches separated by a distance equal to the radiation wavelength [9–17]. It should be noted that apart from spontaneous and induced UR, backward Compton scattering by electrons and backward resonant scattering of optical-range laser beam photons by incompletely ionized ions can be used for generating coherent radiation in the X-ray and gamma ranges [18].

An exact analytic description of radiation from relativistic charges in a magnetic field of the undulator system can be obtained using the generalized forms of the Bessel and Airy functions. The description of UR in the planar and helical undulators includes familiar special functions and their relatively simple generalizations, while exact description of radiation in compound magnetic fields consisting of multiperiodic and aperiodic components remains a complicated mathematical problem. These questions were considered in a number of publications [19–31]; however, different analytic results obtained in these works disagreed with one another. Unfortunately, the Bessel coefficients were calculated with errors [20, 31]. Irrespective of this, the results obtained in [24, 25] were contradictory.

Earlier (and probably for the first time), the idea of undulators with fields with complex configurations was proposed in [32–34] for obtaining hard circularly polarized gamma radiation at higher harmonics of UR and its conversion into longitudinally polarized positrons in the medium. In [35], the inverse problem was solved for determining the field distribution in the undulator in which radiation in the direction of the undulator axis was polarized linearly and was strictly monochromatic in the optimal generation conditions. The field of such an undulator is mainly described by the sum of the first and second harmonics.

In this study, we obtained and analyzed explicit expressions for the Bessel coefficients and UR intensities with new magnetic field configurations in undulators with harmonic elliptically polarized magnetic field, which will be referred to as elliptic for brevity (see [36] for details). In the limiting cases, these expressions describe the helical and planar undulators

taking into account the field harmonics and correct some results from [19–31]. The UR spectral intensity with account for energy spread and the sizes of electron beam were verified by independent numerical simulation using the SPECTRA software [37, 38]. The UR intensity for a helical undulator with an antisymmetric field harmonic were compared with experimental data and were found to be in agreement with them [39].

In contrast to [40], in which a particular case of helical undulator with field harmonics was investigated, in this study we obtained analytic expressions for the intensity in the UR spectra in asymmetric elliptical undulators with higher magnetic field harmonics. Using these expressions, we determined the undulator field configuration for generating the dominating third and fifth UR harmonics. We simulate FEL radiation taking into account the field harmonics in the undulator. For this purpose, we apply specially developed numerical program for 3D simulation of FEL radiation and the phenomenological model of the FEL [41–44]. This model permits arbitrary magnetic fields and can easily be realized in Mathematica code for rapid and realistic estimation of the emitted power and the evolution of the bunching coefficients along the FEL axis.

2. UR INTENSITY AND SPECTRUM OF AN ELLIPTICAL UNDULATOR WITH AN ASYMMETRIC MAGNETIC FIELD HARMONIC

The sinusoidal field of an undulator is known to be an idealization of the actual undulator field. The undulator may also contain other fields with a multiple period. These additional fields are usually weak, but the amplitude of the third field harmonic can reach 10% of the amplitude of main field H_0. This affects the UR structure [39]. Such undulators can increase the radiation power of higher harmonics and amplification factors as in gyrodevices with two-frequency bunching, in which the degree of electron bunching increases due to the constructive interaction at two different harmonics [45–47]. For example, in [48], an optimization of laser operation due to trapping electron bunches by the high-frequency electromagnetic field was proposed. In experiment [39], the KAERI undulator was used with magnetic field

$$\begin{gathered}\mathbf{H} = H_0(\sin(k_\lambda z) - d\sin(hk_\lambda z),\\ \cos(k_\lambda z) + d\cos(hk_\lambda z), 0),\\ h = 1,2,3,\ldots;\end{gathered} \tag{1}$$

in our case, we use parameters $h = 3$, $d = 0.0825$, $k_\lambda = 2\pi/\lambda_u = 2.21622$, $\lambda_u = 2.3$ cm being the undulator period. The resonance wavelengths of radiation emitted by electrons at angle θ to the undulator axis are given by (n is the number of a harmonic)

$$\lambda_n = \frac{\lambda_u}{2n\gamma^2}[1 + k_{\text{eff}}^2 + (\gamma\theta)^2], \tag{2}$$

where

$$\begin{gathered}k_{\text{eff}}^2 = k_{x,\text{eff}}^2 + k_{y,\text{eff}}^2,\\ k_{x,\text{eff}} = k_{y,\text{eff}} = k\sqrt{\frac{1}{2}\left[1 + \left(\frac{d}{h}\right)^2\right]},\\ k = \frac{eH_0}{mc^2}\frac{\lambda_u}{2\pi},\end{gathered} \tag{3}$$

and γ is the Lorentz factor for the electron. Evaluating the spectral density in undulator field (1), we obtain the following exact analytic expressions for the generalized Bessel function:

$$\begin{gathered}J_{n,m}(\xi_1,\xi_2,\xi_3,\xi_4,\xi_5)\\ = \frac{1}{2\pi}\int_{-\pi}^{\pi} d\alpha\exp\{i[n\alpha + \xi_1\cos\alpha + \xi_2\cos(h\alpha)\\ - \xi_3\sin\alpha + \xi_4\sin(h\alpha) - \xi_5\sin((h+1)\alpha)]\},\end{gathered} \tag{4}$$

where

$$\begin{gathered}\xi_1 = \frac{2mk\gamma\theta\cos\varphi}{1 + k^2[1 + (d/h)^2] + \gamma^2\theta^2}, \quad \xi_2 = \frac{d}{h^2}\xi_1,\\ \xi_3 = \xi_1\tan\varphi, \quad \xi_4 = \frac{d}{h^2}\xi_1\tan\varphi,\\ \xi_5 = \frac{mdk^2}{h(h+1)\{1 + k^2[1 + (d/h)^2] + \gamma^2\theta^2\}},\end{gathered} \tag{5}$$

φ is the polar angle in the plane perpendicular to the undulator axis. Using expression (4), we obtain the Bessel coefficients for spontaneous emission of UR harmonics at angle θ to the undulator axis:

$$\begin{gathered}T_{n,x} = \frac{2}{k}\gamma\theta J_{n,n}\cos\varphi + i(J_{n+1,n} - J_{n-1,n})\\ + i\frac{d}{h}(J_{n+h,n} - J_{n-h,n}),\end{gathered} \tag{6}$$

$$\begin{gathered}T_{n,y} = \frac{2}{k}\gamma\theta J_{n,n}\sin\varphi - (J_{n+1,m} + J_{n-1,m})\\ + \frac{d}{h}(J_{n+h,m} + J_{n-h,m}).\end{gathered} \tag{7}$$

These expressions are accounted for in the following expression for the total UR intensity in solid angle Ω:

$$\begin{gathered}\frac{d^2I}{d\omega d\Omega} = \frac{e^2N^2\gamma^2k^2}{c(1 + k_{\text{eff}}^2 + \gamma^2\theta^2)^2}\\ \times\sum_{n=-\infty}^{\infty} n^2\text{sinc}^2\left(\frac{\nu_n}{2}\right)(|T_{n,x}|^2 + |T_{n,y}|^2),\end{gathered} \tag{8}$$

where N is the number of periods in the undulator, $\nu_n = 2\pi nN[(\omega/\omega_n) - 1]$ is the detuning parameter, and $\omega_n = 2\pi c/\lambda_n$ are the UR resonance frequencies. For $\theta = 0$, expression (4) is simplified, arguments $\xi_1, \ldots, \xi_4$

in expression (5) vanish, and only argument ξ_5 is left. For $d = 0$, we obtain a helical undulator:

$$f_{1;x,y} = 1, \quad f_{n\neq 1} = 0,$$

where

$$f_{n;x} = |T_{n,x}|, \quad f_{n;y} = |T_{n,y}|.$$

The KAERI numerical simulation of undulator with field (1) was performed in [39]. Some preliminary estimates of possible radiation from a FEL with such an undulator were obtained in [40, 44].

One of the main source of loss in the UR and broadening of its spectral lines is energy spread σ_e of the electron beam and the deflection of electrons from the undulator axis through angle θ. These factors can be accounted for by evaluating integral

$$\int_{-\infty}^{\infty} \frac{d^2 I(\nu_n + 2\pi n N\varepsilon, \theta)}{d\omega d\Omega} \frac{1}{\sqrt{2\pi}\sigma_e} \exp\left(-\frac{\varepsilon^2}{2\sigma_e^2}\right) d\varepsilon.$$

The calculation of radiation characteristics and evolution of power of harmonics in the FEL is a more complicated and cumbersome problem. It is usually performed in computer programs in which the equations of motion, and the radiation field equations are solved for each harmonic. This takes a long time, special software, and personnel prepared for operating it. A rapid estimate can be obtained using a phenomenological model calibrated and verified in experiments with FELs [41–44]. A generalization of the phenomenological model for elliptical undulators was given in [40]. An attempt at connecting analytically the degree of ordering of the spontaneous radiation spectral lines with the degree of amplification of the corresponding FEL harmonics was made in [49], where an approximate correlation between losses in spontaneous and induced radiations was established.

3. ANALYSIS OF THE EFFECT OF THE THIRD FIELD HARMONIC ON THE RADIATION OF A PLANAR TWO-FREQUENCY UNDULATOR

In this section, we generalize the results of investigations performed in [19–31]. In contrast to the analytic formalism of the generalized Bessel functions, which makes it possible to analyze radiation of undulators with almost any magnetic field configuration, numerical calculation with available programs is possible for several relatively simple undulator field configurations. For example, using the SPECTRA code [37, 38], one can calculate numerically the UR with magnetic field

$$\mathbf{H} = H_0(0, \sin(k_\lambda z) + d\sin(hk_\lambda z), 0), \quad k_\lambda = 2\pi/\lambda_u, \quad h = 1, 2, 3, \ldots . \tag{9}$$

Using harmonics of field $\mathbf{H}$, one can increase or decrease the power of the UR higher harmonics depending on the choice of d and h in expression (9) [20, 23–25, 31]. The UR resonances with field (9) correspond to wavelengths (2), where

$$k_{\text{eff}} = \frac{k}{\sqrt{2}}\sqrt{1 + \left(\frac{d}{h}\right)^2}.$$

Exact calculations of URs with field (9) leads to the following generalized Bessel functions:

$$J_{n,m}(\xi_m, \xi_m^{(i)}) = \frac{1}{2\pi}\int_0^{2\pi} d\varphi \cos\{n\varphi + \xi_m^{(1)}\sin\varphi + \xi_m^{(2)}\sin(\varphi h) + \xi_m^{(3)}\sin[\varphi(h-1)] + \xi_m^{(4)}\sin[\varphi(h+1)] + \xi_m^{(5)}\sin(2\varphi h) + \xi_m \sin 2\varphi\}, \tag{10}$$

where

$$\xi_m \cong \frac{1}{4}\frac{mk^2}{1 + \frac{k^2}{2}\left(1 + \frac{d^2}{h^2}\right) + (\gamma\theta)^2},$$

$$\xi_m^{(1)} = \frac{8\xi_m\gamma\theta}{k}\cos\varphi, \quad \xi_m^{(2)} = \frac{d\xi_1}{h^2}, \quad \xi_m^{(3)} = \frac{4d\xi_m}{h(h-1)}, \tag{11}$$

$$\xi_m^{(4)} = \frac{4d\xi_m}{h(h+1)}, \quad \xi_m^{(5)} = \frac{d^2\xi_m}{h^3}.$$

These functions form the amplitudes of the UR intensity for harmonics with number $n = 1, 2, 3, 4, 5, \ldots$:

$$T_{n,x} = J_{n-1,n} + J_{n+1,n} + \frac{d}{h}(J_{n+h,n} + J_{n-h,n}) + \frac{2\gamma\theta\cos\varphi}{k}J_{n,n}, \tag{12}$$

$$T_{n,y} = \frac{2\gamma\theta\sin\varphi}{k}J_{n,n}.$$

For a conventional planar undulator, we have $d = 0$, and T_n is reduced to conventional Bessel functions $J_n(\xi_0 \equiv \xi|_{d=0})$, which give the well-known Bessel coefficients on the undulator axis:

$$f_n = J_{\frac{n-1}{2}}(-\xi_0) + J_{\frac{n+1}{2}}(-\xi_0).$$

The intensity of spontaneous emission of UR electron in field (9) [22, 23] is described by expression (8) with account for (12).

Additional constant magnetic field components were correctly accounted for in [30].We do not consider here the betatron oscillations emerging due to a deflection of the electron beam from the field axis. In [44], it was proposed that a phenomenological angle be introduced proceeding from the beam geometry, which gives realistic estimates.

We compared the intensities of the UR harmonics in a wide range of the field strength of the undulator third harmonic. The results were obtained analytically using formulas (10) and (11) (see left graphs in Figs. 1–6) as well as numerically using the SPECTRA code (right graphs in Figs. 1–6). Calculations were performed for $N = 150$ periods for better discerning the UR spectra. The amplitude of the third harmonic of

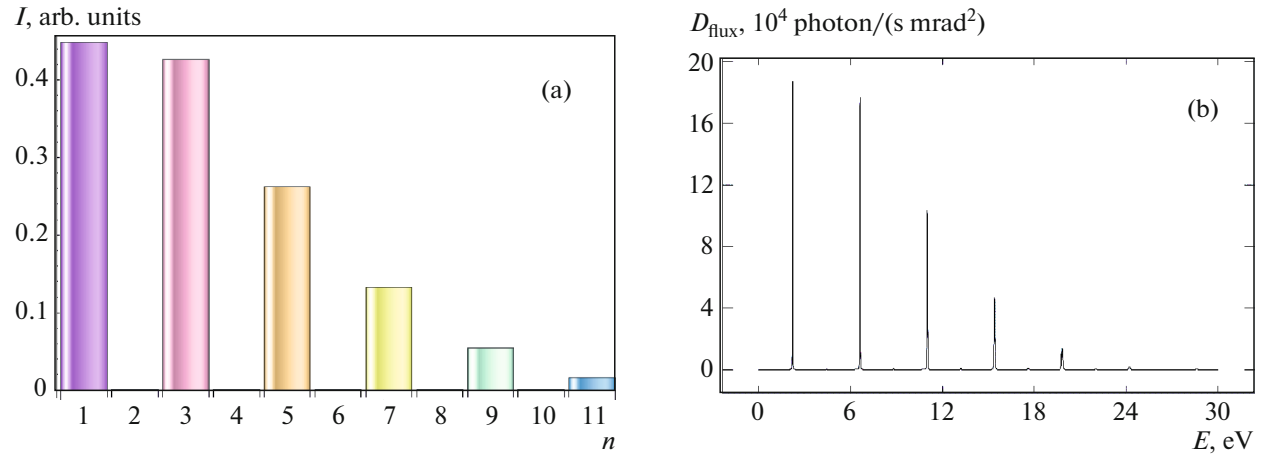

Fig. 1. (Color online) (a) Intensities of UR harmonics in an undulator with $k = 2.133$, $h = 3$, $d = 0.73$, $\sigma_e = 0.9 \times 10^{-3}$ and (b) energy dependence of the photon flux density D_{flux} (the spectral bandwidth is 0.1% of energy in electronvolts).

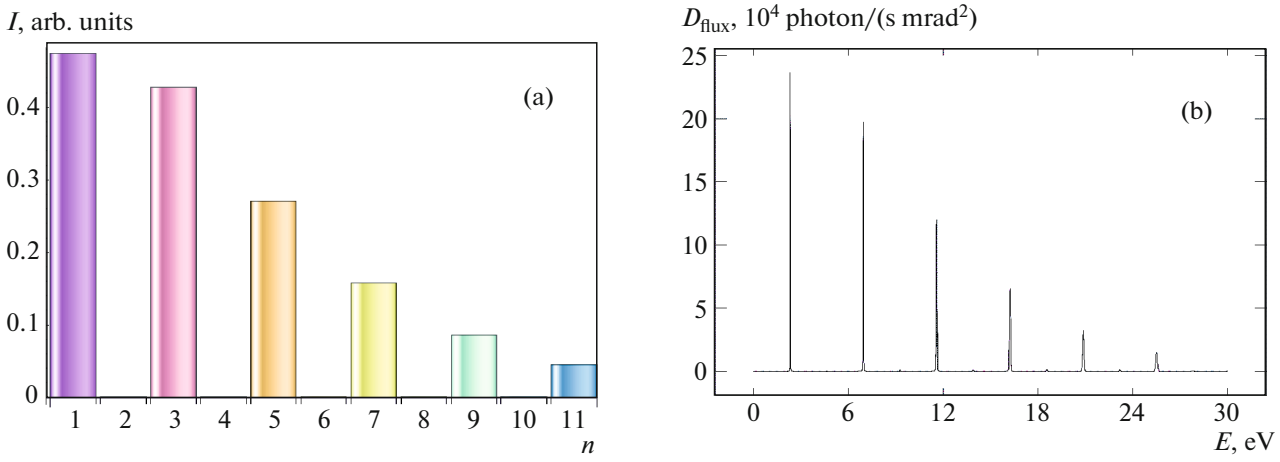

Fig. 2. (Color online) Same as in Fig. 1, but for $d = 0.41$.

the undulator field is determined by ratio d of the field strength for the second component to the strength H_0 of the main field in expression (9) ($d = -1.22$, -0.41, -0.244, 0, 0.41, 0.73).

The parameters of the beam and undulator are as follows: electron energy $E_e = 151.9$ MeV, $\gamma = 297.26$, electron beam power $P_E = 8.05$ GW, current density $J = 4.35 \times 10^8$ A/m^2, full beam cross section $\Sigma_{\text{full}} = 1.219 \times 10^{-7}$ m^2, current $I_0 = 53$ A, electron energy spread $\sigma_e = 0.0009$, undulator parameter $k = 2.1$, and undulator period $\lambda_u = 2.8$ cm.

Numerical and analytic results are in good agreement (see Figs. 1–6), which substantiates our approach. A slight quantitative discrepancy for the very strong third field harmonic with $d = -1.22$ in Fig. 6 is due to the fact that the SPECTRA code apparently accounts for relatively weak perturbations of the fundamental undulator field, while the analytic formalism extends beyond this perturbation range. Formulas (10)–(12) and other expressions given below can be used for analyzing and estimating the single-pass FEL radiation with a high gain (e.g., using the phenomenological model [40–44] and its further evolution in [50], which was verified in FEL experiments).

4. ANALYSIS OF THE EFFECT OF THE THIRD FIELD HARMONIC ON THE RADIATION SPECTRUM OF AN ELLIPTICAL TWO-FREQUENCY UNDULATOR

The quality of the UR spectral line depends on the electron beam. For an undulator with field (1), we chose, in accordance with [39], the following parame-

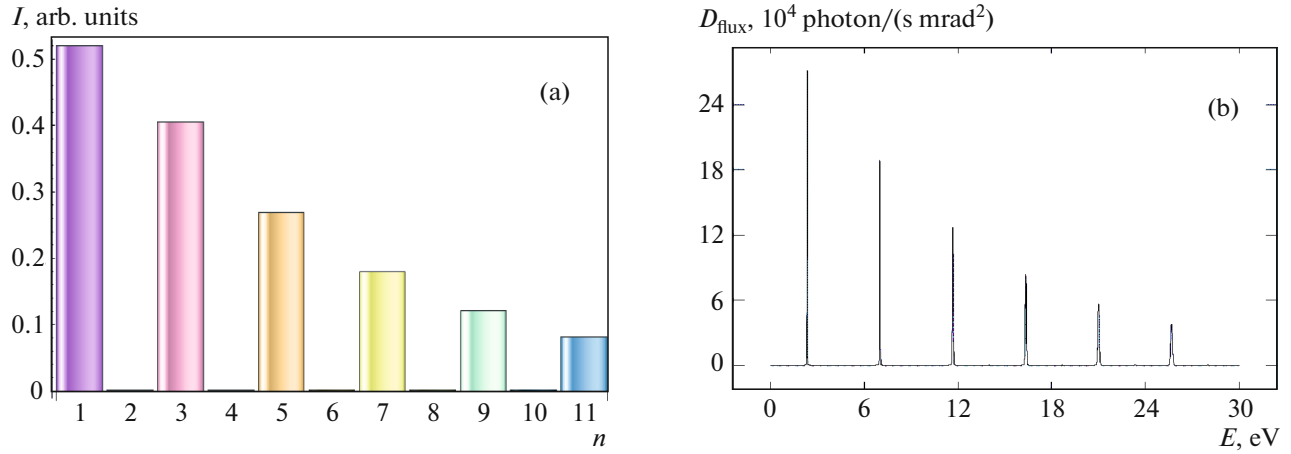

Fig. 3. (Color online) Same as in Fig. 1, but for $d = 0$.

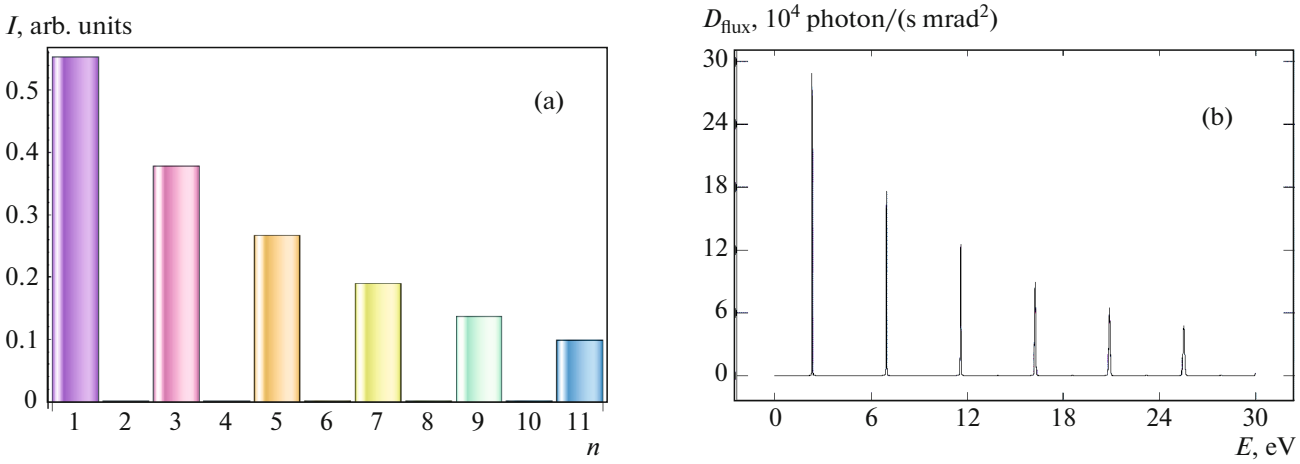

Fig. 4. (Color online) Same as in Fig. 1, but for $d = -0.244$.

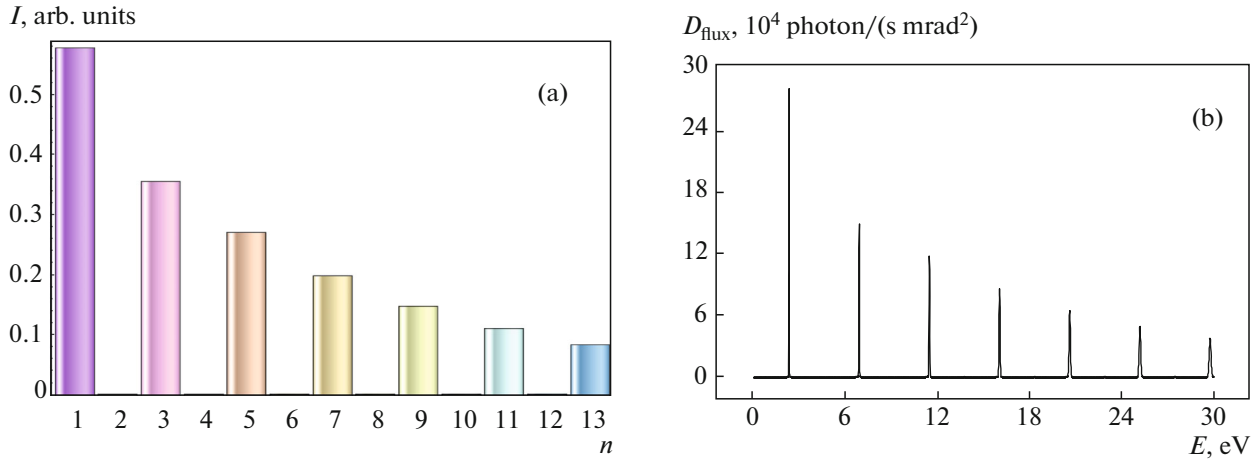

Fig. 5. (Color online) Same as in Fig. 1, but for $d = -0.41$.

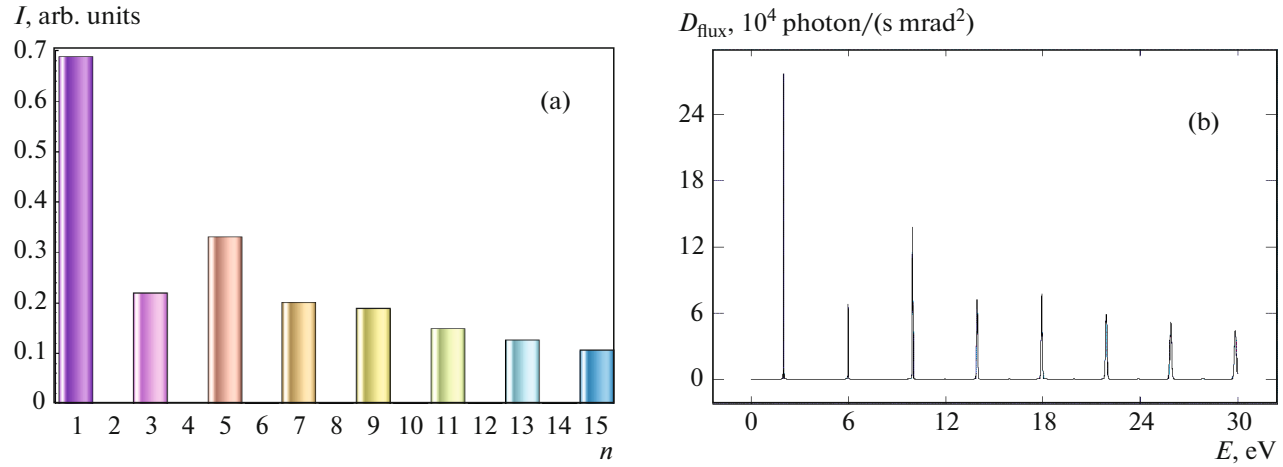

Fig. 6. (Color online) Same as in Fig. 1, but for $d = -1.22$.

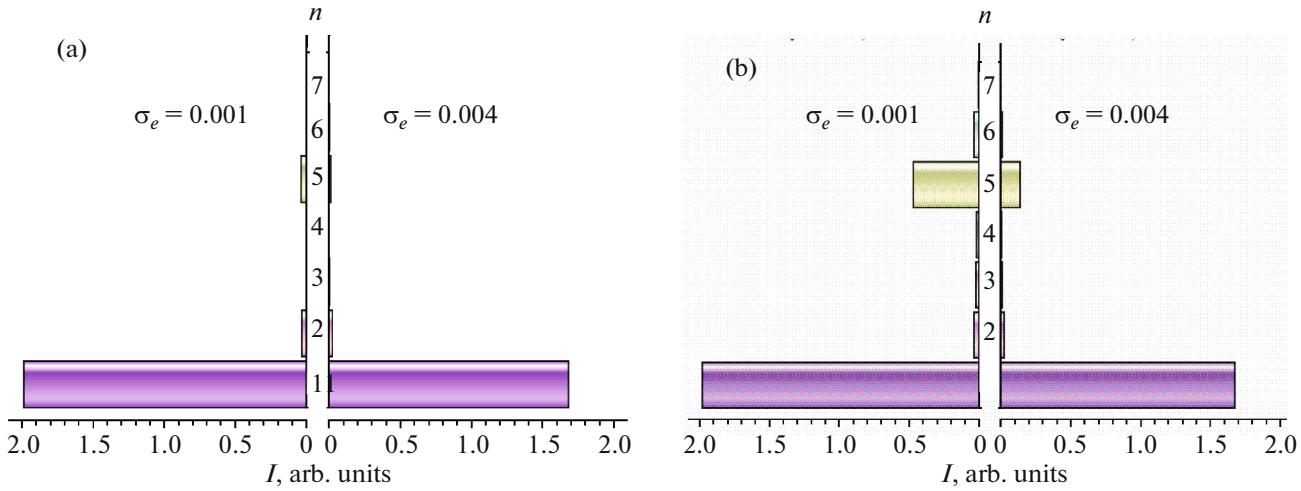

Fig. 7. (Color online) Intensity of UR harmonics with field (1) on the axis with account for the electron energy spread: $d = 0.0825$ (a) and $d = 0.3$ (b); $\gamma = 12.72$; estimates for energy spread are $\sigma_e = 0.001$ and 0.004, respectively.

ters: $\lambda_u = 2.3$ cm, $N = 30$, $k = 2.21622$, $h = 3$, $d = 0.0825$, electron energy $E_e = 6.5$ MeV, $\gamma = 12.72$, emittances $\varepsilon_x = 1.5$ mm mrad and $\varepsilon_y = 0.35$ mm mrad, Twiss parameters $\beta_x = 43.66$ cm and $\beta_y = 28.75$ cm, and divergence angles $\theta_x = 4.5$ mrad and $\theta_y = 1.6$ mrad. The expected UR intensity with account for the electron energy spread in the beam is shown in Fig. 7. Since the beam has finite transverse size and divergence, there appear even harmonics that are not observed in the ideal case. The second harmonic is noticeable and constitutes 2–3% of the first harmonic (see Fig. 7), which is in agreement with [39]. The fifth radiation harmonic was also detected and amounted to approximately 1.7–2.0% of the fundamental tone. It is characterized by a higher power as compared to the third UR harmonic.

We also considered the case of field (1) with $d = 0.3$ and compared the relative powers (see Fig. 7). The shape of the UR lines can be demonstrated analogously to the case considered in [22–30] (we omit this aspect for brevity).

Let us consider an undulator with field (1) and the beam from the SACLA experiment: $\gamma = 1570$, emittance $\varepsilon_{norm} = 3$ mm mrad/γ, and Twiss parameter $\beta = 0.4$ m [29] (Fig. 8).

Both polarizations of radiation have identical intensities of harmonics; for this reason, only one diagram illustrates them. The intensity of the second harmonic reaches 10% of the intensity of the first harmonic (Fig. 8). The intensity of the fifth harmonic constitutes 15% for $d = 0.3$ in field (1) of the first harmonic intensity (Fig. 8b). Other higher harmonics are also presented. In this case, the fifth harmonic prevails in spontaneously emitted radiation.

It would be interesting to consider a FEL with an undulator analogous to that in KAERI: near the undu-

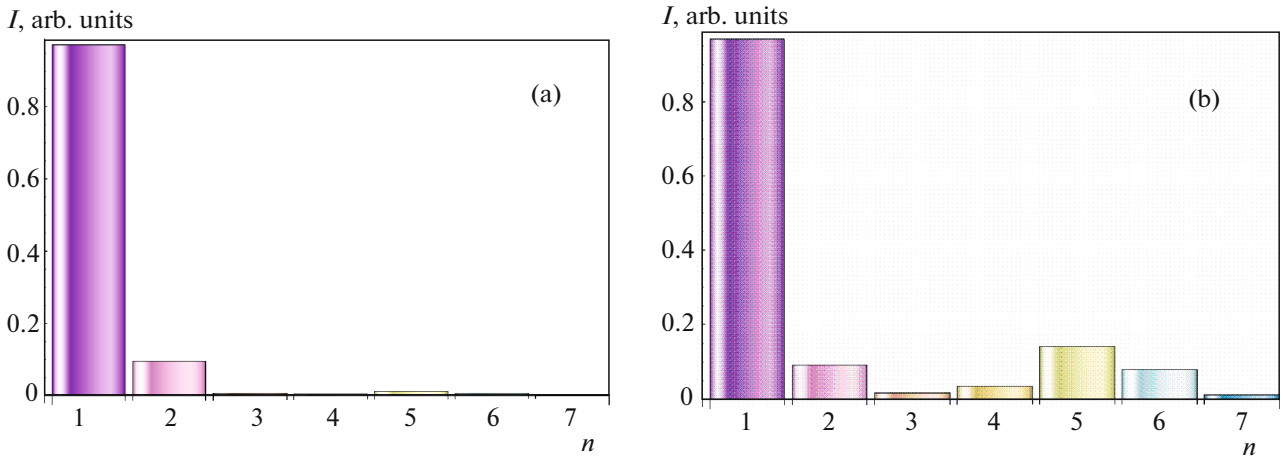

Fig. 8. (Color online) Intensity of UR harmonics with field (1) on the axis for $d = 0.0825$ (a) and $d = 0.3$ (b); $\gamma = 1570$, $\varepsilon_{norm} = 3 \times 10^{-6}$ mm mrad, and $\beta = 0.4$ m.

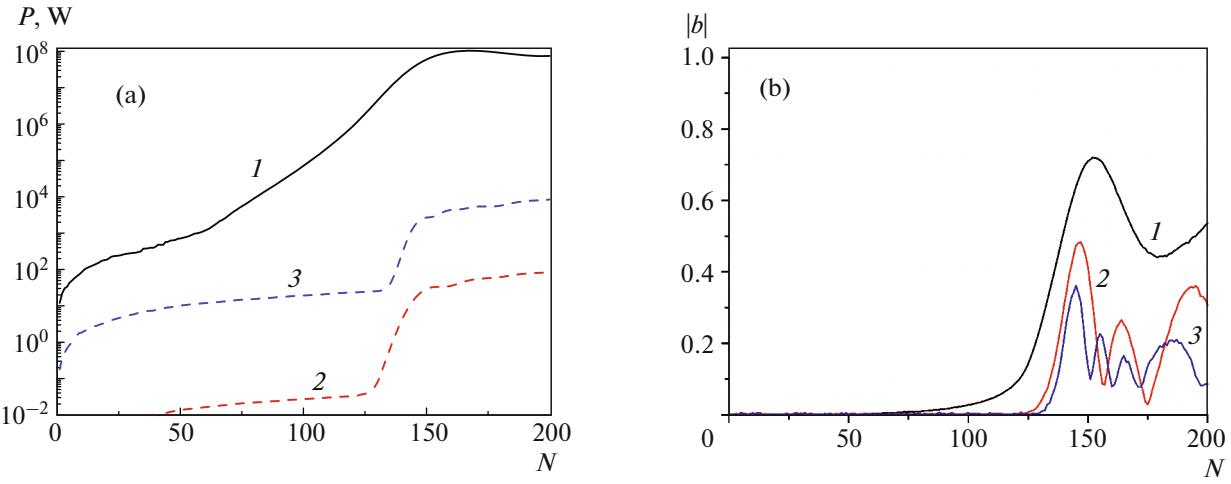

Fig. 9. (Color online) Evolution of (a) power of harmonics and (b) electron bunching coefficient depending on number N of the period of the FEL with undulator field (1) in the self-amplified spontaneous emission (SASE) regime with $\gamma = 300$, $\sigma_e = 0.02 \times 10^{-2}$; $\varepsilon_{norm} = 2$ μm rad, $\beta = 2$ m, $I_0 = 100$ A, $\lambda_u = 3$ cm, $k = 3.5$, $d = 0.3$, $h = 3$; $n = 1$ (*1*), $n = 3$ (*2*), and $n = 5$ (*3*).

lator axis, both polarizations make identical contributions to the intensity of each harmonic. We developed a program of 3D simulation of FEL radiation for this undulator with parameters $k = 3.5$, $d = 0.3$, and $h = 3$. We obtained a laser in which the fifth harmonic of radiation prevails over the third harmonic (Fig. 9).

The fundamental tone dominates because the Bessel coefficient for the first harmonic is almost equal to unity. For $d = 0$, we obtain a helical undulator in which only the first harmonic on the axis is generated.

5. ANALYSIS OF RADIATION OF A TWO-FREQUENCY ELLIPTICAL UNDULATOR

Let us consider the following nontrivial magnetic field configuration of an undulator with multiple periods:

$$\mathbf{H} = H_0(\sin(k_\lambda z), \quad d_1 \sin(hk_\lambda z) + d_2 \cos(lk_\lambda, z), 0), \quad l \neq h, \quad h = 1, 2, 3, \ldots . \tag{13}$$

In the limit $d_1 = 0$, $d_2 \neq 0$ and $d_1 \neq 0$, $d_2 = 0$, formula (13) describes the field of an elliptical undulator. The expressions for the Bessel coefficients for undulators with a harmonic elliptically polarized magnetic field are represented in the best way in [35]. For $d_1 = h = 1$, we obtain a planar undulator, while for $d_1 = 0$ and $d_2 = l = 1$, we have a helical undulator.

In magnetic field configuration (13), the conventional sinusoidal field exists on the x axis like in a planar undulator, while on the y axis, we have a combination of fields of multiple frequencies with the sine and cosine. It should be specified at the very outset that the expressions given below hold for $l \neq h$. Such a field

combination is convenient because it is a generalization of elliptical undulators with the sin–sin and sin–cos configurations of fields. For $d_2 = 0$, we have the sin–sin configuration, while for $d_1 = 0$, we accordingly have the sin–cos configuration. The analytic formalism follows from the general approach described, for example, in [20, 35]. It includes the separation of the oscillating part in the exponential the expression for the spectral intensity, which becomes a generalized Bessel function after certain manipulations with indices and series.

In calculating UR in field (13), we obtain the following generalized Bessel functions:

$$J_n^m(\xi_1,\xi_2,\xi_3,\xi_4,\xi_5,\xi_6,\xi_7,\xi_8) = \frac{1}{2\pi}\int_{-\pi}^{\pi} d\alpha \exp\{i[n\alpha + \xi_1\sin(h\alpha) + \xi_2\cos(l\alpha) + \xi_3\sin\alpha + \xi_4\sin(2\alpha) + \xi_5\sin(2h\alpha) + \xi_6\sin(2l\alpha) + \xi_7\cos((l+h)\alpha) + \xi_8\cos((l-h)\alpha)]\}, \quad (14)$$

where

$$\xi_4 = \frac{1}{4}\frac{mk^2}{1+\frac{k^2}{2}\left[1+\left(\frac{d_1}{h}\right)^2+\left(\frac{d_2}{l}\right)^2\right]+\gamma^2\theta^2}, \quad (15)$$

$$\xi_1 = \frac{8d_1}{kh^2}\gamma\theta\xi_4\cos\varphi, \quad \xi_2 = \frac{8d_2}{kl^2}\gamma\theta\xi_4\cos\varphi,$$
$$\xi_3 = \frac{8}{k}\gamma\theta\sin\varphi\xi_4, \quad \xi_5 = \frac{d_1^2}{h^3}\xi_4, \quad \xi_6 = -\frac{d_2^2}{l^3}\xi_4, \quad (16)$$
$$\xi_7 = \frac{4d_1d_2}{hl(l+h)}\xi_4, \quad \xi_8 = \frac{4d_1d_2}{hl(l-h)}\xi_4.$$

Amplitudes $T_{n;\,x,\,y}$ for the x- and y-polarizations of UR have form

$$T_{n,x} = \frac{2}{k}\gamma\theta J_n^n\cos\varphi + \frac{d_1}{h}(J_{n+h}^n + J_{n-h}^n) + i\frac{d_2}{l}(J_{n+l}^n - J_{n-l}^n), \quad (17)$$

$$T_{n,y} = \frac{2}{k}\gamma\theta J_n^n\sin\varphi + (J_{n+1}^n + J_{n-1}^n), \quad (18)$$

where $J_n^m \equiv J_n^m(\xi_{1,2,3,4,5,6,7,8}(m))$ (see expression (14)). For the wavelengths of UR resonances (8), we are using effective undulator parameter

$$k_{\text{eff}}^2 = \frac{k^2}{2}\left[1+\left(\frac{d_1}{h}\right)^2+\left(\frac{d_2}{l}\right)^2\right], \quad (19)$$

where $k = H_0\lambda_u e/2\pi m_e c^2$ and the total intensity is defined by expression (8) combined with (9). For most setups, $\gamma\theta \sim 10^{-2}$ and $(\gamma\theta)^2 \ll 1$. For $d_1 = 0$, $d_2 = 1$, and $l = 1$, we obtain a helical undulator with Bessel coefficients $T_{1;\,x,\,y} = 1$ and $T_{n\neq 1} = 0$.

Let us consider an undulator with field

$$\mathbf{H} = H_0(\sin(k_\lambda z), \sin(3k_\lambda z) + 0.3\cos(k_\lambda z), 0),$$

i.e., in expression (13), $h = 3$, $l = 1$, $d_1 = 1$, and $d_2 = 0.3$. In this case, UR exhibits quite interesting features. Let us choose $k = 2.21622$ and $\lambda_u = 0.023$ m like in [39] and consider a beam with $\gamma = 11.8$, $\varepsilon_{\text{norm}} = 0.925/\gamma$ mm mrad, and $\beta = 0.37$ m. This gives the following values of Bessel coefficients $f_{n,\,x}$ and $f_{n,\,y}$:

$$f_{x;n=1,\ldots,11} = \left\{\begin{matrix}\mathbf{0.347327}, 0.00460441, \mathbf{0.295931}, 0.00249113, \mathbf{0.224602}, 0.00214126,\\ 0.145829, 0.00234819, 0.0935949, 0.00233896, 0.0636811\end{matrix}\right\}, \quad (20)$$

$$f_{y;n=1,\ldots,11} = \left\{\begin{matrix}\mathbf{0.79742}, 0.0018173, \mathbf{0.394852}, 0.00215424, \mathbf{0.191188}, 0.00239025,\\ 0.0986364, 0.00215422, 0.0602848, 0.00173364, 0.0429623\end{matrix}\right\} \quad (21)$$

(the harmonics making predominant contributions to radiation are given in bold type). It should be noted that Bessel coefficient $f_{x;\,1} \approx \mathbf{0.35}$ for the fundamental tone in the x-polarization in expression (20) is close to Bessel coefficient $f_{x;\,3} \approx \mathbf{0.30}$ for the third harmonic, and the fifth harmonic also has a close value of the Bessel coefficient ($f_{x;\,5} \approx \mathbf{0.22}$). Dimensionless intensities of UR harmonics are shown in Fig. 10.

Pay attention to the right diagram in Fig. 10. The intensities of the third and fifth UR harmonics with the x-polarization are more than three times higher than the intensity of the fundamental tone with the corresponding polarization, and the third harmonic in the y-polarization is also more intense than the fundamental tone.

For generating higher UR harmonics, it is expedient to use field (13) with $h = 3$, $l = 1$, $d_1 = 1$, and $d_2 = 0.25$. The corresponding Bessel coefficients for the x-polarization are given by

$$f_{x;n=1,\ldots,11} = \left\{\begin{matrix}\mathbf{0.291609}, 0.00426642, \mathbf{0.279681}, 0.00217237, \mathbf{0.217977}, 0.00196355,\\ 0.145185, 0.00224461, 0.0969743, 0.00229411, 0.0688733\end{matrix}\right\}. \quad (22)$$

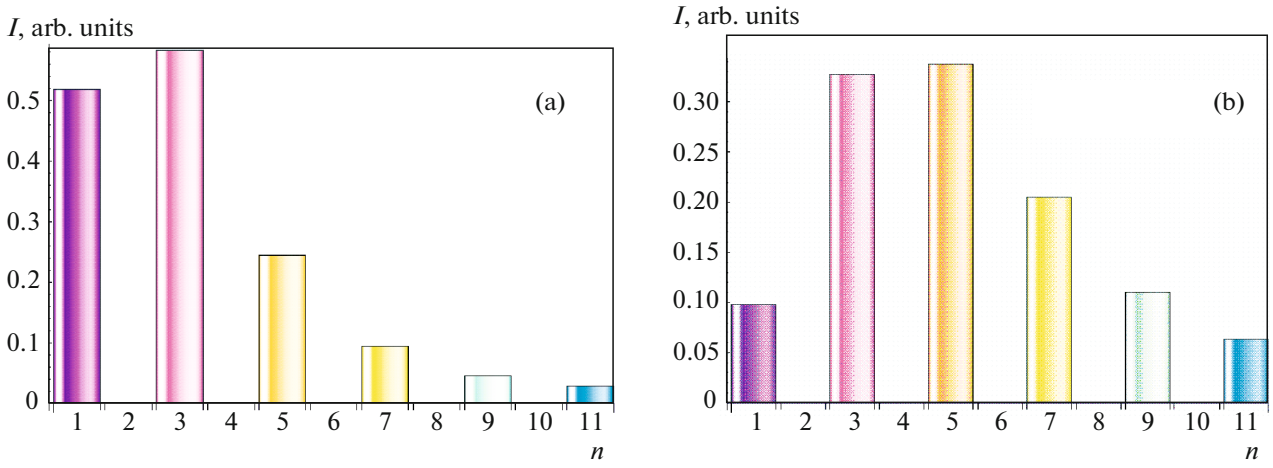

Fig. 10. (Color online) Intensity of UR harmonics with field (13) on the axis with account for emittance and energy spread for $k = 2.21622$, $h = 3$, $d_1 = 1$, $d_2 = 0.3$, $l = 1$, $\sigma = 0.9 \times 10^{-3}$, and $N = 150$ for (a) y-polarization and (b) x-polarization.

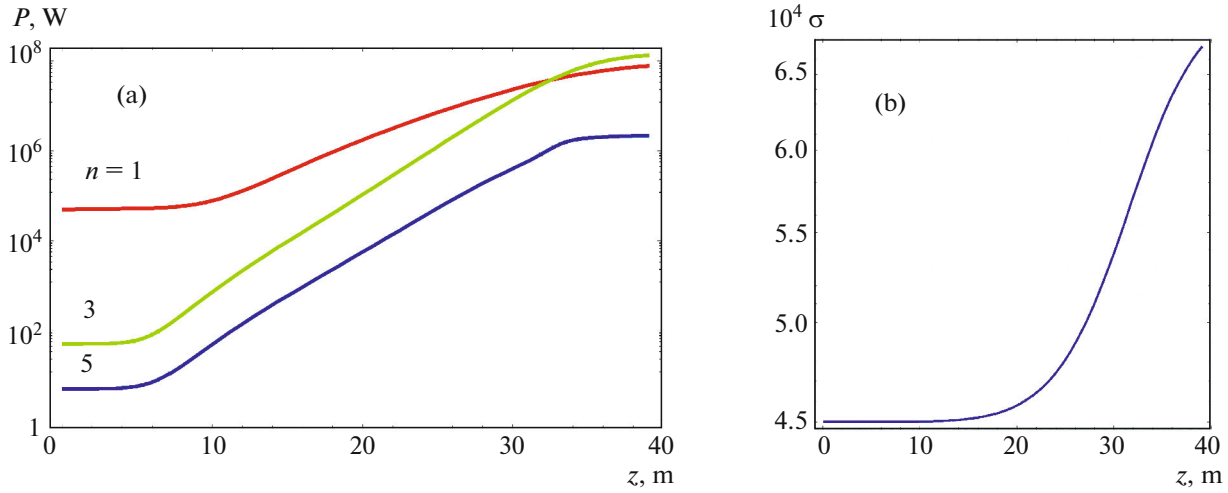

Fig. 11. (Color online) Estimate of power of the x-polarized radiation for (a) $n = 1, 3, 5$ and (b) evolution of the electron energy spread along the FEL axis with an elliptical undulator with field (13); $h = 3$, $d_1 = 1$, $d_2 = 0.25$, $l = 1$, $k = 2.216$, $\lambda_u = 2.3$; electron beam parameters from the SACLA experiment: $\gamma = 1570$, $I = 300$ A, $\sigma_e = 4.5 \times 10^{-4}$, $\beta = 5$ m, and $\varepsilon_{x,y} = 3$ mm mrad.

In the y-polarization of radiation, the fundamental tone prevails; we assume that this polarization can be filtered out. The evolution of the power of the x-polarization of radiation and of the electron energy spread over the length of the FEL undulators, which was obtained using the phenomenological model [40], is illustrated in Fig. 11. The power of the FEL third harmonic with wavelength $\lambda_3 = 6$ nm increases faster than the power of the fundamental tone with $\lambda_1 = 18$ nm. Their values attain saturation approximately over one length of the undulator. The third harmonic is generated in the linear regime up to saturation, and the saturation power of this harmonic is even slightly higher than the fundamental tone power. The energy spread caused by the fundamental tone in this polarization is small. This example demonstrates that elliptical biharmonic undulators can be used in FELs for generating polarized harmonics with a high radiation power without resorting to a phase shift for suppressing the fundamental tone.

6. CONCLUSIONS

In this study, we have considered undulator radiation in multiperiodic undulators and have derived rigorous analytic expressions for the Bessel coefficients and the UR intensity with account for the electron energy spread using the formalism of generalized Bessel functions. We have compared the analytic results

for some undulators with our numerical results obtained using the SPECTRA code and have obtained good agreement between them.

For radiation of a helical undulator with the antisymmetric higher harmonic of field (1), we have obtained exact analytic expressions for the Bessel coefficients and radiation intensity with account for the geometry of actual beams. Our results agree well with experiment. The intensity of the UR second harmonic amounts to 2–3% on the intensity of the first harmonic, because of the finite beam size. We have shown that the weak third harmonic of the undulator field (about 10% of fundamental field H_0, $d = 0.1$, $h = 3$) generates the fifth harmonic in the UR spectrum. Its radiation power amounts to less than 2% of the fundamental tone power, which is in conformity with experiment. The stronger third harmonic ($d = 0.3$) ensures the UR fifth harmonic power at a level of 10–25% of the fundamental tone power. The second harmonic of the FEL radiation is due to the finite size and focusing of the electron beam.

We have analyzed the radiation of an elliptical biharmonic undulator with magnetic field (13). We have derived exact analytic expressions for the Bessel coefficients and UR harmonic intensities in terms of the generalized Bessel functions. We have determined parameters $h = 3$, $l = 1$, $d_1 = 1$, and $d_2 = 0.3$ for the elliptical biharmonic undulator, which give small values of the Bessel coefficients for the fundamental tone in the x-polarization and at the same time large values of the Bessel coefficients for the UR third and fifth harmonics. In the spectrum of spontaneous radiation of this undulator in the x-polarization, the fifth harmonic has the highest power; the power of the third harmonic is lower, while the first harmonic is found to be weak. In the y-polarization, the third harmonic has the highest power, and the power of the first harmonic is lower. The simulation of the single-pass FEL with such an undulator shows that the power of the third harmonic of radiation with the x-polarization has reached the fundamental tone power at the end of the FEL without using the phase shift and suppression of the increase in the fundamental harmonic.

Thus, our analysis of radiation of elliptical biharmonic undulators demonstrates certain advantages of such undulators over conventional undulators in the generation of harmonics and makes it possible to introduce them into further investigation based on the exact analytic expressions derived in this study.

ACKNOWLEDGMENTS

The authors thank A.V. Borisov and V.Ch. Zhukovskii for fruitful discussions.

FUNDING

One of the authors (A.M.K) is grateful to the “Basis” Foundation for Development of Theoretical Physics and Mathematics for the support of this study.

REFERENCES

1. L. A. Artsimovich, and I. Ya. Pomeranchuk, Zh. Eksp. Teor. Fiz. **16**, 379 (1946).
2. V. L. Ginzburg, Izv. Akad. Nauk SSSR, Ser. Fiz. **11**, 1651 (1947).
3. H. Motz, W. Thon, and R. N. J. Whitehurst, Appl. Phys. **24**, 826 (1953).
4. D. F. Alferov, Yu. A. Bashmakov, and E. G. Bessonov, Sov. Tech. Phys. **18**, 1336 (1973).
5. D. F. Alferov, Yu. A. Bashmakov, and P. A. Cherenkov, Sov. Phys. Usp. **32**, 200 (1989).
6. V. G. Bagrov, G. S. Bisnovatyi-Kogan, and V. A. Bordovitsyn, *Theory of Radiation of Relativistic Particles* (Fizmatlit, Moscow, 2002) [in Russian].
7. V. G. Bagrov, I. M. Ternov, and B. V. Kholomai, *Radiation of Relativistic Electrons in a Longitudinal Periodic Electric Field of a Crystal* (TFSO AN SSSR, Tomsk, 1987) [in Russian].
8. N. A. Vinokurov and E. B. Levichev, Phys. Usp. **58**, 850 (2015).
9. B. W. J. McNeil and N. R. Thompson, Nat. Photon. **4**, 814 (2010).
10. C. Pellegrini, A. Marinelli, and S. Reiche, Rev. Mod. Phys. **88**, 015006 (2016).
11. Z. Huang and K. J. Kim, Phys. Rev. ST Accel. Beams **10**, 034801 (2007).
12. E. L. Saldin, E. A. Schneidmiller, and M. V. Yurkov, *The Physics of Free Electron Lasers* (Springer, Berlin, Heidelberg, 2000).
13. R. Bonifacio, C. Pellegrini, and L. Narducci, Opt. Commun. **50**, 373 (1984).
14. P. Schmüser, M. Dohlus, J. Rossbach, and C. Behrens, *Free-Electron Lasers in the Ultraviolet and X-Ray Regime*, Springer Tracts Mod. Phys. (Springer Int., Swith-erland, 2014).
15. C. Pellegrini, Phys. Scr. **2016**, 014004 (2016).
16. G. Margaritondo and P. R. Ribic, J. Synchrotr. Rad. **18**, 101 (2011).
17. G. Margaritondo, Riv. Nuovo Cim. **40**, 411 (2017).
18. W. Placzek, A. Abramov, S. E. Alden, et al., in *Proceedings of the 25th Cracow Epiphany Conference on Advances in Heavy Ion Physics, Jan. 8–11, 2019, Cracow, Poland*, arxiv:1903.09032.
19. K. Zhukovsky, J. Opt. **20**, 095003 (2018).
20. G. Dattoli, V. V. Mikhailin, P. L. Ottaviani, and K. Zhukovsky, J. Appl. Phys. **100**, 084507 (2006).
21. G. Dattoli, A. Doria, L. Giannessi, and P. L. Ottaviani, Nucl. Instrum. Methods Phys. Res., Sect. A **507**, 388 (2003).
22. K. V. Zhukovsky, Mosc. Univ. Phys. Bull. **70**, 232 (2015).
23. K. Zhukovsky, Laser Part. Beams **34**, 447 (2016).

24. J. Hussain and G. Mishra, Nucl. Instrum. Methods Phys. Res., Sect. A **656**, 101 (2011).
25. G. Mishra, M. Gehlot, and J.-K. Hussain, Nucl. Instrum. Methods Phys. Res., Sect. A **603**, 495 (2009).
26. K. Zhukovsky, Nucl. Instrum. Methods Phys. Res., Sect. B **369**, 9 (2016).
27. K. Zhukovsky, J. Appl. Phys. **122**, 233103 (2017).
28. K. V. Zhukovsky, Russ. Phys. J. **60**, 1630 (2017).
29. K. Zhukovsky, Opt. Commun. **353**, 35 (2015).
30. K. Zhukovsky, J. Electromagn. Wave **29**, 132 (2015).
31. Q. Jia, Phys. Rev. ST Accel. Beams **14**, 060702 (2011).
32. E. G. Bessonov, PhIAS Preprint No. 18 (Phys. Inst. Acad. Sci. USSR, Moscow, 1982).
33. V. I. Alekseev and E. G. Bessonov, in *Proceedings of the 6th All-Union Workshop on Use of Synchrotron Radiation SR-84* (IYaF SO AN SSSR, Novosibirsk, 1984), p. 92.
34. E. G. Bessonov, Nucl. Instrum. Methods Phys. Res., Sect. A **282**, 405 (1989).
35. V. I. Alexeev and E. G. Bessonov, Nucl. Instrum. Methods Phys. Res., Sect. A **308**, 140 (1991).
36. A. A. Kolomenskii, I. V. Sinil'shchikova, E. G. Bessonov, et al., Tr. FIAN **214**, 193 (1993).
37. T. Tanaka, Phys. Rev. ST Accel. Beams **17**, 060702 (2014).
38. T. Tanaka and H. Kitamura, J. Synchrotr. Rad. **8**, 1221 (2001).
39. K. Lee, J. Mun, S.-H. Park, et al., Nucl. Instrum. Methods Phys. Res., Sect. A **776**, 27 (2015).
40. K. Zhukovsky, Res. Phys. **13**, 102248 (2019).
41. K. Zhukovsky and A. Kalitenko, J. Synchrotr. Rad. **26**, 159 (2019).
42. K. Zhukovsky and A. Kalitenko, J. Synchrotr. Rad. **26**, 605 (2019).
43. K. Zhukovsky, J. Opt. **20**, 095003 (2018).
44. K. V. Zhukovsky and A. M. Kalitenko, Russ. Phys. J. **62**, 354 (2019).
45. A. V. Savilov and G. S. Nusinovich, Phys. Plasmas **14**, 053113 (2007).
46. G. S. Nusinovich and O. Dumbrajs, Phys. Plasmas **2**, 568 (1995).
47. A. V. Savilov and G. S. Nusinovich, Phys. Plasmas **15**, 013112 (2008).
48. E. D. Belyavskii, I. A. Goncharov, and A. A. Silivra, J. Exp. Theor. Phys. **81**, 724 (1995).
49. K. Zhukovsky, J. Phys. D **50**, 505601 (2017).
50. K. Zhukovsky, J. Synchrotr. Rad. **26**, 1481 (2019).

Translated by N. Wadhwa